ELSEVIER

Journal of Organometallic Chemistry 495 (1995) 33–39

Journal of Organometallic Chemistry

Substitution of SO_2 for CO in triruthenium carbonyl anions

G.B. Karet, C.L. Stern, J.A. Cody, S.J. Lange, M.A. Pell, C. Slebodnick, D.F. Shriver *

Department of Chemistry, Northwestern University, Evanston, IL 60208-3113, USA

Received 22 April 1994; in revised form 18 November 1994

Abstract

The cluster $[PPN]_2[Ru_3(CO)_{11}]$ (**I**) reacts with SO_2 to give $[PPN]_2[Ru_3(CO)_9SO_2]$ (**II**) and $[PPN]_2[Ru_3(CO)_7(SO_2)_3]$ (**III**). Both **II** and **III** were characterized by IR spectroscopy and ^{13}C NMR spectroscopy, and $[Et_4N]_2[Ru_3(CO)_9SO_2]$ was characterized by single-crystal X-ray diffraction. In both **II** and **III**, SO_2 exhibits the μ_3,η^2 bonding mode, and **III** has two additional SO_2 ligands bridging two metals through sulfur. The latter SO_2 disposition is also indicated by spectroscopic studies for $[Et_4N][HRu_3(CO)_9(SO_2)_2]$, which was formed by the reaction of $[Et_4N][HRu_3(CO)_{11}]$ with SO_2. Spectroscopic data indicate that the SO_2 ligand in **II** is acetylated by $CH_3C(O)Cl$. Crystallographic data for $[Et_4N]_2[Ru_3(CO)_9SO_2]$: space group $P2_1/c$, $a = 19.937(4)$Å, $b = 10.074(3)$Å, $c = 20.010(3)$Å, $\beta = 113.63(1)°$.

Keywords: Ruthenium; Sulfur dioxide; Metal clusters; Carbonyl; Carbon monoxide; X-ray structure

1. Introduction

Carbonyl-stretching frequencies and electrochemical studies suggest that in a series of iron clusters, SO_2 is a better π acceptor ligand than CO [1,2]. Thus SO_2 may form many monometallic and dimetallic complexes with metals in low oxidation states. In monometallic complexes, SO_2 displays a rich array of bonding modes, including coplanar coordination, η^1 pyramidal coordination, and η^2 coordination, in which SO_2 binds through both sulfur and oxygen (Fig. 1) [3,4]. In dimetallic complexes, SO_2 may also bridge two metals through sulfur, as in $[CpFe(CO)_2]_2SO_2$ [5], or, on rare occasions, through both sulfur and oxygen, as in $[Mo(CO)_2(py)(SO_2)(PPh_3)_2]$ [6]. Monometallic and dimetallic complexes with SO_2 ligands have been extensively studied [3,7], but SO_2 cluster complexes with three or more metals are less common [1,2,8,9]. The bonding of SO_2 to clusters is of interest, because SO_2 is known to bind to the surface of metallic Fe, Pt, Rh, Ru, and Ni, and then transform to surface-bound S^{2-} and $[SO_4]^{2-}$ [10,11].

The clusters $[PPN][HFe_3(CO)_9SO_2]$, $[Rh_4(CO)_4(SO_2)_3(P(OPh)_3)_4]$ [12], and $[Pd_5(SO_2)_2(PR_3)_5]$ (R = Me) [13] display the μ_3,η^2 bonding mode. Sulfur dioxide clusters have been synthesized by addition of SO_2 to formally unsaturated clusters [14], by SO_2 oxidation of anionic clusters [1], and most often by substitution of SO_2 for other ligands [1,2,8]. Because the ruthenium clusters $[HRu_3(CO)_{11}]^-$ and $[Ru_3(CO)_{12}]$ readily un-

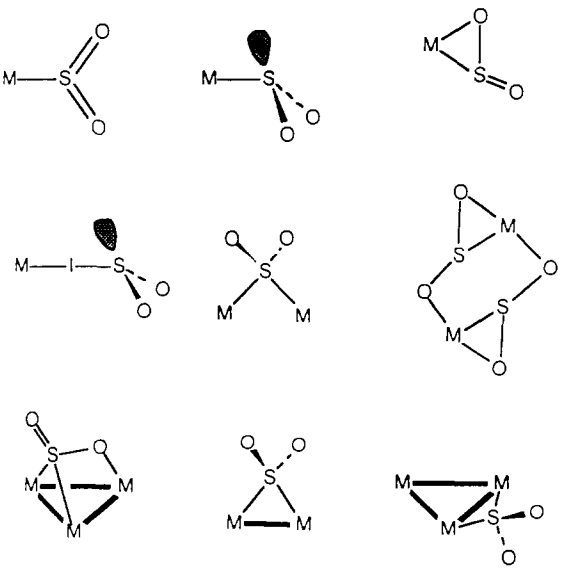

Fig. 1. Some bonding modes of SO_2 in monometallic, dimetallic, and cluster complexes.

* Corresponding author.

SSDI 0022-328X(94)05341-3

dergo ligand substitution reactions [15,16], triruthenium clusters were chosen as precursors for the synthesis of new electron-rich SO_2 complexes. Two of the resulting clusters contain μ_3, η^2-SO_2 ligands.

2. Experimental details

2.1. General

All manipulations were carried out with standard Schlenk techniques under a prepurified N_2 atmosphere or on a high vacuum line [17]. Solids were handled in the oxygen-free N_2 atmosphere of a drybox. Solvents were distilled from appropriate drying agents before use [18]. Solution IR spectra were recorded on a Bomem MB-Series FTIR spectrometer at 2 cm^{-1} resolution. IR spectra of solids were recorded using Nujol mulls between KBr plates. The ^1H and ^{13}C NMR spectra of ^{13}C-labeled compounds were acquired on a Varian XL-400 or Varian Unity 400+ spectrometer operating at 400 MHz for ^1H and 100 MHz for ^{13}C. Before use, CD_2Cl_2 was vacuum distilled from P_4O_{10} and D_8-THF from Na. These solvents served as internal NMR references. FAB mass spectra, obtained by Cs^+ bombardment of samples in an m-nitrobenzyl alcohol matrix, were recorded by Dr. Hung of Northwestern University Analytical Services Laboratory. Elemental analysis was done by Elbach Analytical Laboratories, Engelskirchen, Germany.

Sulfur dioxide was freeze-thaw degassed before use. Acetyl chloride was distilled from PCl_5 and quinoline before use. The clusters $[PPN]_2[Ru_3(CO)_{11}]$ and $[Et_4N][HRu_3(CO)_{11}]$ were prepared by published procedures [19,20]. To maximize the yield of the SO_2 complex, $[PPN]_2[Ru_3(CO)_{11}]$ was used within two weeks of synthesis.

2.2. Synthesis of $[PPN]_2[Ru_3(CO)_9(SO_2)]$

To 140 mg (0.0829 mmol) of $[PPN]_2[Ru_3(CO)_{11}]$, 9 ml of CH_2Cl_2 was added. The solution was freeze-thaw degassed, and SO_2, 0.0912 mmol, 1.1. equivalents, was added on the high vacuum line. The solution was stirred for 1 h, during which time evolution of 1.4 equivalents of CO was observed. The solution darkened rapidly to a brown color, and then gradually lightened to orange. The solvent was removed under vacuum to produce a yellow oil. Yellow microcrystals of $[PPN][Ru_3(CO)_9SO_2]$ were grown by addition of 40 ml of Et_2O to a solution of the cluster in 10 ml acetone. These were isolated by filtration and dried under vacuum. Yield 92 mg, 65%. In a similar manner, $[Et_4N]_2[Ru_3(CO)_9SO_2]$ was synthesized from $[Et_4N]_2[Ru_3(CO)_{11}]$ dissolved in CH_3CN. IR νCO, THF 2016 (w), 1957 (vs), 1928 (s), 1900 (m), 1775 (m). IR, νSO, nujol 1089 (s), 892 (s). ^{13}C NMR, 20°C, δ, ppm from TMS, CD_2Cl_2, 211.95; −90°C, CD_2Cl_2 209.6(7), 214.3(2). Anal. Calc.: C 57.3, H 3.54, N 1.65, S 1.89, Ru 17.9. Found: C 56.89, H 4.14, S 2.10, Ru 18.90%.

2.3. Synthesis of $[PPN]_2[Ru_3(CO)_7(SO_2)_3]$

To 350 mg (0.207 mmol) of $[PPN]_2[Ru_3(CO)_{11}]$, 10 ml of CH_2Cl_2 was added. The solution was freeze-thaw degassed, and three equivalents of SO_2 were added. The solution was stirred overnight, during which time it turned from orange-red to yellow-orange. After removal of the CH_2Cl_2 under vacuum, the cluster was dissolved in acetone and filtered to remove insoluble light-yellow solids. The acetone was removed in vacuo, and a dark-yellow solution of the cluster was extracted with 10 ml of THF. Yellow-orange microcrystals were grown by dropwise addition of pentane to a solution of the THF extract in 5 ml of acetone. Yield 50 mg, 14%. IR, CH_2Cl_2, νCO 2048(m), 2015(vs), 1981(s), 1853(w, br). IR, nujol, ν; νSO 1074(w), 1040(s), 978(w). FAB-MS $P = 693$ ($R_p = 0.023$ for the mass range 687–696 amu), with loss of three carbonyls and two SO_2 ligands. ^{13}C NMR, δ, ppm from TMS, −90°C, CD_2Cl_2 229.28(1), 197.73(2), 197.45(2), 195.95(1), 193.60(1). Anal. Calc.: C 53.6, H 3.39, N 1.59, S 5.43, Ru 17.1. Found: C 54.3, H 3.83, N 1.62, S 5.23, Ru 17.15%.

2.4. Synthesis of $[Et_4N][HRu_3(CO)_9(SO_2)_2]$

Sulfur dioxide (1.23 mmol, 3.04 equivalents) was condensed on a previously degassed solution of 300 mg (0.404 mmol) of $[Et_4N][HRu_3(CO)_{11}]$ in 15 ml of THF. The mixture was warmed to room temperature and allowed to stir for 5 h. Gas evolved, and the color of the solution changed from red-orange to orange. This solution was filtered to remove suspended orange solids, and dropwise addition of pentane to the filtrate produced orange microcrystals, which were isolated by filtration and dried under vacuum. Yield 170 mg, 52%. IR, νCO, THF 2116 (vw), 2079 (m), 2044 (vs), 2015 (w), 1990 (m); vSO, nujol 1044 (s), 1021 (m). FAB-MS $P = 686$ m/z ($R = 0.010$ for $P \pm 7$ amu) with loss of one SO_2 and eight carbonyls. ^1H NMR, THF, 20°C, −15.68 ppm from TMS. ^{13}C NMR, 25°C, THF, δ, ppm from TMS, 199.22(2), $J_{C-C} = 3$ Hz; 198.65(4), $J_{C-H} = 4$ Hz; 194.64(1), J_{C-C}, 3 Hz; 193.65(2). Analy. Calc.: C 25.1, H 2.6, N 1.7, S 7.86, Ru 37.2. Found: C 24.72, H 2.54, N 1.83, S 8.04, Ru 38.50%.

2.5. Reaction of $[PPN]_2[Ru_3(CO)_9SO_2]$ with SO_2

To a 50 mg (0.029 mmol) sample of $[PPN]_2[Ru_3(CO)_9SO_2]$, 5 ml CH_2Cl_2 was added. The solution was freeze-thaw degassed, cooled to −196°C, and 1.1 equivalent of SO_2 was added. After the solution was

allowed to warm to room temperature and then stirred for 10 min, its color turned from yellow to red. Further stirring overnight produced a light-orange solution and 3.1 equivalents of CO. An IR spectrum of the reaction mixture matched that of $[PPN][Ru_3(CO)_7(SO_2)_3]$. The solvent was removed, and the cluster was dissolved in 7 ml of acetone. Dropwise addition of diethyl ether gave orange microcrystals. Yield, 25 mg, 49%.

2.6. Reaction of $[PPN]_2[Ru_3(CO)_9SO_2]$ with AcCl

In a 5 mm NMR tube, $[PPN]_2[Ru_3(CO)_9SO_2]$, ca. 50 mg, was dissolved in CD_2Cl_2. Acetyl chloride, 30 μl, was added, whereupon the solution turned from orange to yellow. At 20°C the ^1H NMR spectrum contained a single peak of 2.19 ppm, ppm from TMS and the ^{13}C NMR, spectrum contained peaks at 186.4, 166.9, 22.5, ppm from TMS.

2.7. Crystal Structure of $[Et_4N]_2[Ru_3(CO)_9SO_2]$

A yellow plate-like crystal of $[Et_4N]_2[Ru_3(CO)_9SO_2]$ was grown by slow diffusion of pentane into a solution of the cluster in acetone. It was mounted on a glass fiber using oil (Paratone-N, Exxon) and was transferred to the cold stream (−120°C) of an Enraf-Nonius CAD-4 diffractometer. A summary of the data collection is given in Table 1. Unit cell constants were determined by least-squares refinement of the setting angles of 25 unique reflections. Lorenz polarization and an analytical absorption correction were applied with transmission factors between 0.77 and 0.88.

Calculations were performed with the TEXSAN 5.0 crystallographic software package. The structure was solved by direct methods (SHELXS-86), with full-matrix least-squares refinement. All non-hydrogen atoms were refined with anisotropic thermal parameters. Hydrogen atoms were fixed in idealized positions. The maximum peak in the final difference map was 1.26 e^- Å^{-3} (in the vicinity of the metal positions) and the minimum peak −0.80 e^- Å^{-3}. Final positional parameters for significant atoms are shown in Table 2.

Table 1
X-ray crystal structure data for $[Et_4N]_2[Ru_3(CO)_9SO_2]$

Formula	$Ru_3SO_{11}N_2C_{25}H_{40}$
M	937.95
Crystal size, mm	0.43×0.19×0.09
Crystal system	monoclinic
Space group	$P2_1/c$(#14)
a, Å	19.937(4)
b, Å	10.074(3)
c, Å	20.010(3)
β, deg	113.63(1)
V, Å^3	3682(3)
Z	4
d (calc), g·cm^{-3}	1.692
μ(Mo Kα), cm^{-1}	13.02
Radiation	Mo Kα (λ = 0.71069 Å)
Scan type	ω-θ
2θ max, deg.	48.0
Unique data	6150
Observed data, (I) > 3σ(I)	3803
Number of variables	415
Reflection/parameter ratio	9.16
$R(F)$	0.043
$Rw(F)$	0.046
GOF	1.60

Table 2
Positional parameters of significant atoms for $[Et_4N]_2[Ru_3(CO)_9SO_2]$

Atom	x	y	z
Ru(1)	0.84835(3)	0.22783(7)	0.29730(4)
Ru(2)	0.72752(3)	0.23554(7)	0.33444(3)
Ru(3)	0.74380(4)	0.02384(7)	0.25403(4)
S(1)	0.8066(1)	0.0595(2)	0.3833(1)
O(1)	0.8101(3)	−0.0227(8)	0.4442(4)
O(2)	0.8843(3)	0.1069(5)	0.3953(3)
O(11)	1.0016(3)	0.3283(7)	0.3300(4)
O(12)	0.7904(3)	0.3978(7)	0.1634(3)
O(13)	0.8705(3)	0.0017(6)	0.2021(3)
O(14)	0.8370(3)	0.4660(6)	0.3913(3)
O(21)	0.6779(3)	0.2926(7)	0.4563(3)
O(22)	0.6296(4)	0.4411(7)	0.2272(4)
O(23)	0.5931(3)	0.0501(7)	0.2634(4)
O(31)	0.7237(5)	−0.2720(8)	0.2379(5)
C(11)	0.9440(5)	0.2888(8)	0.3191(5)
C(12)	0.8119(4)	0.331(1)	0.2149(5)
C(13)	0.8412(4)	0.0513(9)	0.2352(4)
C(14)	0.8158(4)	0.367(1)	0.3607(4)
C(21)	0.6965(4)	0.2703(9)	0.4097(5)
C(22)	0.6659(5)	0.363(1)	0.2666(5)
C(23)	0.6525(4)	0.0811(9)	0.2788(4)
C(31)	0.7303(5)	−0.160(1)	0.2438(6)
C(32)	0.6889(5)	0.066(1)	0.1547(5)

3. Results and Discussion

The cluster $[PPN]_2[Ru_3(CO)_{11}]$ (**I**) reacts with an equimolar quantity of SO_2 by ligand substitution reactions produces the cluster $[PPN]_2[Ru_3(CO)_9SO_2]$, **II**, and free CO. Reaction with three equivalents of SO_2 leads to the formation $[PPN]_2[Ru_3(CO)_7(SO_2)_3]$, **III**, with further evolution of CO (Eqs. 1 and 2).

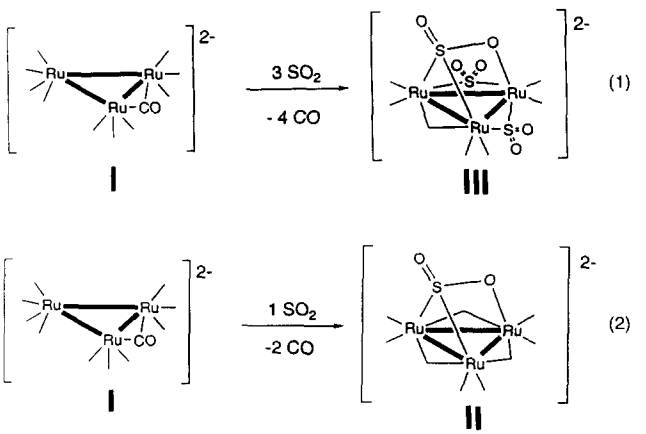

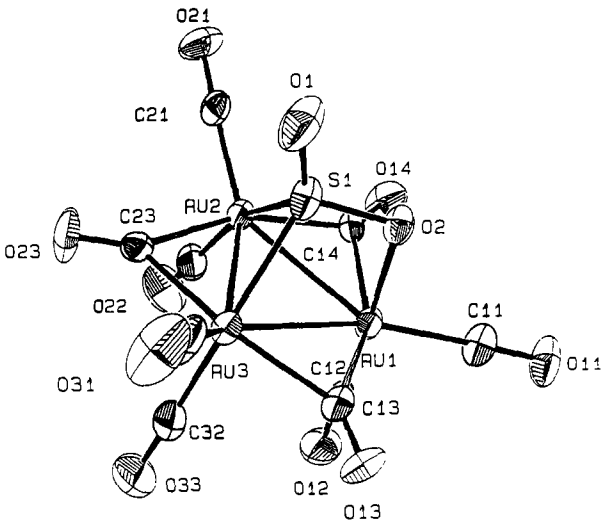

Fig. 2. ORTEP drawing of the cluster anion in $[Et_4N]_2[Ru_3(CO)_9SO_2]$. Ellipsoids are shown at the 50% probability level.

Addition of only one equivalent of SO_2 to **II** leads to isolation of only $[PPN]_2[Ru_3(CO)_7(SO_2)_3]$ (**III**). However, the sequence of color changes from red to yellow suggests that $[PPN]_2[Ru_3(CO)_8(SO_2)_2]$ may form as an unstable intermediate, indicated in Eq. 3.

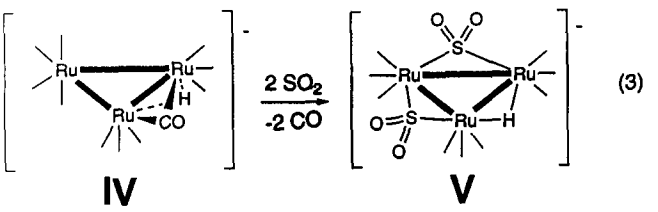

(3)

3.1. Characterization of the $[Ru_3(CO)_9SO_2]^{2-}$ anion

An ORTEP drawing of the $[Et_4N]_2$ $[Ru_3(CO)_9SO_2]$, Fig. 2, reveals that the SO_2 ligand bridges three metals through sulfur and oxygen. The sulfur binds to two ruthenium atoms, and the third ruthenium is bound to the oxygen. This SO_2 coordination mode is also found in $[PPN][HFe_3(CO)_9SO_2]$ [2], $[Rh_4(CO)_4(SO_2)_3(P(OPh)_3)_4]$ [12], and $[Pd_5(SO_2)_2(PMe_3)_5]$ [13]. As observed for other clusters, the capping SO_2 ligand in $[Et_4N]_2$ $[Ru_3(CO)_9SO_2]$ may be regarded as a formal four-electron donor [2,12,13]. The structure of $[Et_4N]$-$[Ru_3(CO)_9SO_2]$ is most closely related to that of $[PPN][HFe_3(CO)_9SO_2$ [2]. Both trimetallic clusters contain an SO_2 ligand that caps the metal triangle. However, $[Et_4N]_2[Ru_3(CO)_9SO_2]$ contains bridging carbonyl ligands and $[PPN][HFe_3(CO)_9SO_2]$ does not [2].

The three Ru–Ru distances (Table 3) range from 2.768(1) Å to 2.806(1) Å, in a nearly equilateral triangle. The Ru–O bond (2.172(5) Å) is 0.1 Å shorter than the Rh–O bond in $[Rh_4(CO)_4(SO_2)_3(P(OPh)_3)_4]$ [12]. The Ru–S distances (2.313(2), 2.407(3) Å) are similar to that in $[Ru(CO)_2(\eta^2\text{-}SO_2 \cdot SO_2)]$(2.363(1) Å) [21]. The distance between S and the Ru-bound O (1.545(5) Å) is close to the longest S–O distances in mononuclear complexes with η^2-SO_2 ligands [21]. However, the short distance, 1.452(7) Å, is similar to the S–O distance in free SO_2 (1.43 Å) [22].

Table 3
Selected bond distances in $[Et_4N]_2[Ru_3(CO)_9SO_2]$

atom–atom	distance (Å)	atom–atom	distance (Å)
Ru1–Ru2	2.792(1)	Ru1–Ru3	2.806(1)
Ru2–Ru3	2.768(1)	Ru1–O2	2.172(5)
Ru2–S1	2.313(2)	Ru3–S1	2.407(3)
S1–O1	1.452(7)	S1–O2	1.545(5)
Ru1–C11	1.881(8)	Ru1–C12	1.84(1)
Ru1–C13	2.141(9)	Ru1–C14	2.158(9)
Ru2–C14	2.094(9)	Ru2–C21	1.877(8)
Ru2–C22	1.91(1)	Ru2–C23	2.136(8)
Ru3–C31	1.87(1)	Ru3–C32	1.89(1)
Ru3–C23	2.149(8)		
O11–C11	1.151(9)	O12–C12	1.16(1)
O13–C13	1.158(9)	O14–C14	1.16(1)
O21–C21	1.154(9)	O22–C22	1.14(1)
O23–C23	1.142(9)	O31–C31	1.14(1)
O33–C32	1.14(1)		

Bond angles, Table 4, show that the long S–O bond in $[Et_4N]_2$ $[Ru_3(CO)_9SO_2]$, as in $[PPN][HFe_3(CO)_9$-$SO_2]$, lies nearly parallel to the plane of the metal triangle [2]. The Ru1–O2–S1 angle is 94.9(3)°. As in $[PPN][HFe_3(CO)_9SO_2]$, coordination of the SO_2 ligand to the metal triangle narrows the O–S–O angle (109.7(3)°) by about 10° from that in free SO_2 [23]. The decrease in the OSO angle is consistent with metal-to-ligand π donation [7].

A Mull IR spectrum of $[PPN]_2[RU_3(CO)_9SO_2]$ (**II**) contains low frequency S–O stretches characteristic of SO_2 bound to metals through both sulfur and oxygen [23]. The S–O stretch in **II** at 892 cm^{-1} is the lowest found so far in clusters (Table 5). This low frequency is attributed to the delocalization of electron density from the Ru_3 dianion into an S–O antibonding orbital of the μ_3, η^2 SO_2 ligand, and it suggests that the SO_2 ligand in **II** may be especially susceptible to electrophilic

Table 4
Selected bond angles for $[Et_4N]_2[Ru_3(CO)_9So_2]$

atom–atom–atom	angle (deg)	atom–atom–atom	angle (deg)
Ru2–Ru1–Ru3	59.27(3)	Ru2–Ru1–O2	77.4(1)
Ru3–Ru1–O2	78.6(1)	Ru1–Ru2–Ru3	60.60(2)
Ru1–Ru2–S1	64.96(6)	Ru3–Ru2–S1	55.68(6)
Ru1–Ru3–Ru2	60.13(3)	Ru1–Ru3–S1	52.53(6)
Ru2–S1–Ru3	71.79(7)	Ru2–S1–O1	126.0(3)
Ru2–S1–O2	107.4(2)	Ru3–S1–O1	130.3(3)
Ru3–S1–O2	105.7(2)	O1–S1–O2	109.7(3)
Ru1–O2–S1	94.9(3)		

Table 5
S–O bond distances and νSO for clusters with μ_3,η^2 SO_2 ligands

Cluster	d S–O (Å)	νSO (cm^{-1})
$[PPN][HFe_3(CO)_9SO_2]$ [2]	1.62(1), 1.434(9)	929, 1143
$[Rh_4(CO)_4(SO_2)_3[P(OPh)_3)_4]$ [12]	1.47(1), 1.44(2) 1.43(2), 1.50(2)	1230, 1102 1074, 977
$[Et_4N]_2[Ru_3(CO)_9SO_2]$	1.54, 1.43	892, 1089
$[PPN]_2[Ru_3(CO)_7(SO_2)_3]$	–	978, 1077 1040
$[Pd_5(SO_2)_4(Ph_3As)_5]$ [27]	1.438(7),1.476(7) 1.489(8),1.438(8)	1216, 1196,1066
$[Pd_5(SO_2)_4(PMe_3)_5]$ [13]	–	1262,1057 1184,1162

attack at oxygen, as observed for $[PPN][HFe_3(CO)_9SO_2]$ [2].

The ^{13}C NMR spectrum of **II** at 20°C has one peak at 211.95 ppm, indicating rapid intermetallic CO exchange at room temperature. The peak broadens at 0°C, and, by −60°C, splits into a resonance at 214 ppm, corresponding to two carbonyls, and one at 209 ppm, corresponding to seven carbonyls. At −90°C, these two resonances broaden slightly. The resonance at 214 ppm may correspond to the carbonyls on the ruthenium bonded to the oxygen and the other resonance may correspond to the remaining seven carbonyls. An alternate, but in our opinion less likely possibility, is that precession of the μ_3-SO_2 ligand around the Ru_3 triangle results in scrambling of the carbonyls as seen in an alkynyl bridged triruthenium cluster [24].

3.2. Characterization of $[PPN]_2[Ru_3(CO)_7(SO_2)_3]$ (III)

The S–O IR absorptions in $[PPN]_2[Ru_3(CO)_7(SO_2)_3]$ (**III**) are at 1074, 1040, and 978 cm^{-1}. The strongest band, at 1040 cm^{-1}, is assigned to the bridging SO_2 ligands in **III** [23]. The bands at 1074 cm^{-1} and 978 cm^{-1} suggest a μ_3,η^2-SO_2 ligand is present in **III** [23]. Because the lowest S–O stretch occurs at higher frequency than in **II** or $[PPN][HFe_3(CO)_9SO_2]$ [2], the μ_3,η^2-SO_2 ligand in **III** is probably less electron-rich than in the other two clusters.

The FAB-MS spectrum of $[PPN]_2[Ru_3(CO)_7(SO_2)_3]$, **III**, has a parent peak at 693 m/z. The spectrum contains fragments corresponding to the loss of five carbonyl ligands and two SO_2 ligands from the parent. The isotope distribution of the parent ion also support the formulation of **III** as $[PPN]_2[Ru_3(CO)_9(SO_2)_3]$ (R = 0.023 for the mass range 687–696 amu).

The carbonyl ligands in $[PPN]_2[Ru_3(CO)_7(SO_2)_3]$ do not exchange even at room temperature. The ^{13}C NMR spectrum suggests that the cluster has a plane of symmetry through the capping SO_2 ligand and the O-bound Ru. The structure for the cluster anion of **III** shown in Eq. 1 is based on the ^{13}C NMR and νSO spectra. The carbonyl resonance at 232.0 ppm is assigned to the bridging carbonyl on the ruthenium atoms bridged by sulfur. The presence of a bridging carbonyl is confirmed by an IR band at 1853 cm^{-1} in the solution spectrum of **III**. The ^{13}C NMR resonances at 199.9 ppm and 199.5 ppm, corresponding to two carbonyls each, are assigned to the terminal carbonyls on the ruthenium atoms bridged by sulfur. One of these peaks corresponds to the carbonyls on the same side of the Ru_3 plane as the η^2, μ^3-SO_2 ligand and the other to the carbonyls on the other side of the Ru_3 plane. The remaining two resonances, at 197.7 ppm and 195.7 ppm, belong to the carbonyls on the O-bound Ru.

3.3. Synthesis and characterization of $[Et_4N][HRu_3(CO)_9(SO_2)_2]$ (V)

The cluster $[Et_4N][HRu_3(CO)_{11}]$ (**IV**) reacts with SO_2 to produce $[Et_4N][HRu_3(CO)_9(SO_2)_2]$ (**V**) cleanly and in good yields.

The solution IR spectrum of **V** indicates that no bridging carbonyls are present in the cluster. The mull IR spectrum of the product has two strong S–O stretches at 1201 cm^{-1} and 1044 cm^{-1}, which are in the region for SO_2 ligands bridging two metals through sulfur [23]. A FAB-mass spectrum of **V** supports its formulation as $[Et_4N][HRu_3(CO)_9(SO_2)_2]$. A parent peak occurs at 686 m/z (R = 0.010 for $P \pm 7$ amu) and the loss of one sulfur dioxide and eight carbonyls is evident in the FAB-mass spectrum of **V**.

The ^1H and ^{13}C NMR spectra allow the assignment of the structure of $[Et_4N][HRu_3(CO)_{10}(SO_2)_2]$ (**V**). An ^1H resonance at −15.68 ppm suggests that the hydride ligand bridges two Ru atoms on the cluster. The carbonyl region of the $^{13}C\{^1H\}$ NMR spectrum of partially ^{13}C-enriched **V** at 20°C (Fig. 3) has four resonances, at 199.19 (2 COs), 198.66 (4 COs), 194.64 (1 CO), and 193.65 (2 COs). The ^1H and ^{13}C NMR spectra are temperature independent between −90°C and room

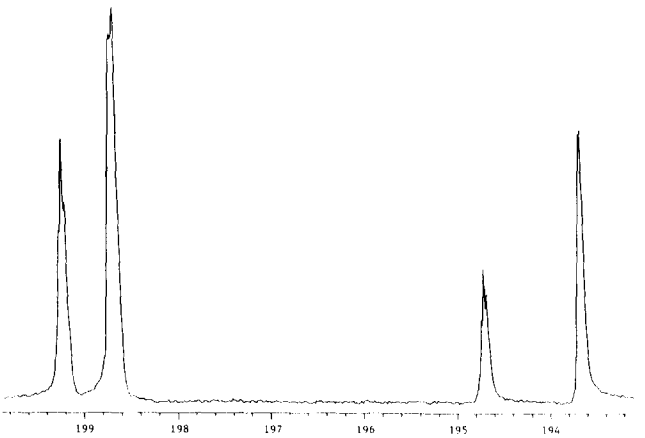

Fig. 3. ^{13}C NMR spectrum of $[Et_4N][HRu_3(CO)_9(SO_2)_2]$.

temperature, with no observed changes in carbonyl exchange. These IR and NMR data suggest that the cluster anion of **V** has the structure shown in Eq. 3.

A plane of symmetry runs through one Ru and bisects the bond between the other two Ru atoms. The resonances at 199.19 ppm and 194.64 ppm are coupled to each other ($J_{C-C} = 3$ Hz), and are assigned to the carbonyls on the Ru bound to both SO_2 ligands. This small coupling is not seen in the natural abundance ^{13}C NMR spectrum of the carbonyl region of **V** and most likely occurs between COs on the same metal rather than between those farther apart on different Ru atoms. The remaining resonances are assigned to the carbonyls on the other two Ru atoms. The feature at 198.66 ppm represents two sets of two equivalent carbonyls that are cisoid to the hydride ligand and that fortuitously overlap. The hydride ligand is thought to span the Ru–Ru bond that is not bridged by sulfur because the ^{13}C NMR data indicate that a plane of symmetry bisects that Ru–Ru bond.

In contrast, the reaction of SO_2 with $[Et_4N][HRu_3(CO)_{11}]$ (Eq. 3) differs from its reaction with $[PPN][HFe_3(CO)_{11}]$ (Eq. 4) [2]. The latter does not undergo multiple substitution in the presence of up to four equivalents of SO_2. Additionally, SO_2 adopts a different bonding mode in **V** than it does in $[PPN][HFe_3(CO)_9SO_2]$ [2].

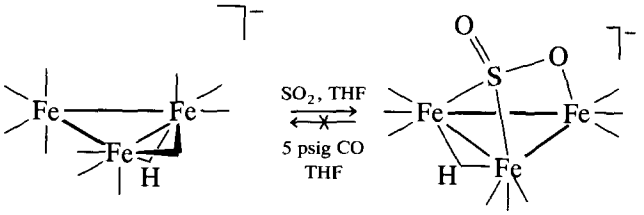

(4)

The carbonyl-stretching bands of the triruthenium SO_2 clusters shift to higher frequencies with substitution of SO_2 for carbonyl ligands. The most intense C–O stretch in $[PPN]_2[Ru_3(CO)_{11}]$ is found at 1945 cm^{-1}. In $[PPN]_2[Ru_3(CO)_9SO_2]$, this band is shifted to 1957 cm^{-1}, and in $[PPN]_2[Ru_3(CO)_9(SO_2)_3]$, to 2015 cm^{-1}. Similarly, the most intense C–O stretch in $[Et_4N][HRu_3(CO)_{11}]$, at 2014 cm^{-1}, is found at 2044 cm^{-1} in $[Et_4N][HRu_3(CO)_9(SO_2)_2]$. These shifts suggest that SO_2 is a stronger electron-withdrawing ligand than CO, and this interpretation is consistent with the changes observed in νCO upon SO_2 substitution for a series of iron clusters [1,2].

3.4. Electrophilic Attack of $[PPN][Ru_3(CO)_9SO_2]$

The reaction of **II** with acetyl chloride leads to formation of a new cluster with ^1H and ^{13}C NMR resonances at 2.19 (^1H), 22.5 (^{13}C), and 166.9 (^{13}C) ppm corresponding to the methyl protons, the methyl carbon, and carbonyl carbon, respectively, of an oxygen-bound acetyl group. These chemical shifts for the acetyl group in $[PPN][Ru_3(CO)_9SO_2Ac]$ (**VI**) are similar to those of other oxygen-bound acetyl groups, such as in $[HFe_3(CO)_9SO_2Ac]$ or $[PPN][Fe_3(CO)_9CCOAc]$ [2,25]. Signals for unreacted AcCl are also observed. A single resonance for the carbonyls occurs at 186.37 ppm, and no downfield resonance characteristic of a carbonyl that has undergone electrophilic attack is observed [26]. Therefore, the most likely site for attack of the acetyl chloride is the oxygen of coordinated SO_2, **VI**, as observed for $[PPN][HFe_3(CO)_9SO_2]$.

3.5. Supplementary Material

A full listing of positional and thermal parameters, complete lists of bond distances and angles, and structure factor tables (43 pages) are available from the authors.

Acknowledgements

This work was supported by the U.S. Department of Energy through grant DE-FG02-ER13640.

References

[1] P.L. Bogdan, M. Sabat, S.A. Sunshine, C. Woodcock and D.F. Shriver, *Inorg. Chem.*, 27 (1988) 1904.
[2] G.B. Karet, C.L. Stern, D.M. Norton and D.F. Shriver, *J. Am. Chem. Soc.*, 115 (1993) 9979.
[3] R.R. Ryan, G.J. Kubas, D.C. Moody and P.G. Eller, *Struct. Bonding (Berlin)*, 46 (1981) 47.
[4] W.A. Schenk, *Angew. Chem., Int. Ed. Engl.*, 26 (1987) 98.
[5] (a)P. Reich-Rohrwig, A.C. Clark, R.L. Downs and A. Wojcicki, *J. Organomet. Chem.*, 145 (1978) 57; (b) M.R. Churchill, B.G. DeBoer and K.L. Kalra, *Inorg. Chem.*, 12 (1973) 1646; (c) M.R. Churchill, B.G. DeBoer, K.L. Kalra, P. Reich-Rohrwig and A. Wojcicki, *J. Chem. Soc., Chem. Commun.*, (1972) 981.
[6] G.J. Jarvinen, G.J. Kubas, R.R. Ryan, *J. Chem. Soc., Chem. Commun.*, (1981) 305.
[7] D.M.P. Mingos, *Trans. Met. Chem. (Weinheim Ger.)*, *3* (1978) 1.
[8] (a) C.E. Briant, D.G. Evans and D.M.P. Mingos, *J. Chem. Soc., Chem. Commun.*, (1982) 1144; (b) C.E. Briant, D.G. Evans and D.M.P. Mingos, *J. Chem. Soc., Dalton Trans.*, (1986) 1535; (c) M.F. Hallam, N.D. Howells, D.M.P. Mingos and R.W.M. Wardle, *J. Chem. Soc., Dalton Trans.*, (1985) 845; (d) D.M.P. Mingos, P. Oster and D.J. Sherman, *J. Organomet. Chem.*, 320 (1987) 257; (e) D.G. Evans, G.R. Hughes, D.M.P. Mingos, J.-M. Bassett and A.J. Welch, *J. Chem. Soc., Chem. Commun.*, (1980) 1255; (f) S.G. Bott, M.F. Hallam, O.J. Ezomo, D.M.P. Mingos and I.D. Williams, *J. Chem. Soc., Dalton Trans.*, (1988) 1461; (g) S.G. Bott, A.D. Burrows, O.J. Ezomo, M.F. Hallam, J.G. Jeffry and D.M.P. Mingos, *J. Chem. Soc., Dalton Trans.*, (1990) 3335; (h) D.C. Moody and R.R. Ryan, *Inorg. Chem.*, 16 (1977) 1052.

[9] D. Braga, R. Ros and R. Roulet, *J. Organomet. Chem.*, 286 (1985) C8.
[10] (a) W.A. Hermann, *Angew. Chem., Int. Ed. Engl.*, 21 (1982) 117; (b) G. Lavigne, H. D. Kaesz, in B.C. Gates, L. Guczi and H. Knozinger (eds.), *Metal Clusters in Catalysis*, Elsevier, New York, 1986; (c) G. Sundarajan, *J. Sci. Ind. Res.*, 48 (1989) 417; (d) M. Thomas, B.F. Beier and E.L. Muetterties, *J. Am. Chem. Soc.*, 98 (1976) 1296.
[11] (a) R.V. Siriwardane and J.M. Cook, *J. Colloid Interface Sci.*, 104 (1985) 251; (b) R.V. Siriwardane and J.M. Cook, *J. Colloid Interface Sci.*, 116 (1987) 463; (c) M. Furuyama, K. Kishi and S. Ikeda, *J. Elect. Spec. Rel. Phenom.*, 13 (1978) 59; (d) L.M. Pecora and P.J. Ficalora, *Metall. Trans., A*8 (1977) 1841; (e) T.D. Wilke, X. Gao, C.G. Takaidis and M.J. Weaver, *J. Catal.*, 130 (1991) 62; (f) H.P. Bonzela and R. Ku, *J. Chem. Phys.*, 59 (1973) 1641; (g) U. Köhler and H.-W. Wassmuth, *Surf. Sci.*, 117 (1982) 668; (h) R.C. Ku and P. Wynblatt, *Appl. Surf. Sci.*, *8* (1981) 250; (i) C.R. Trundle and A.F. Culey, *Faraday Discuss. Chem. Soc.*, 60 (1975) 51.
[12] C.E. Briant, B.R.C. Theopold and D.M.P. Mingos, *J. Chem. Soc., Chem. Commun.*, (1981) 963.
[13] S.G. Bott, O.J. Ezomo and D.M.P. Mingos, *J. Chem. Soc., Chem. Commun.*, (1988) 1048.
[14] (a) G.D. Jarvinen and R.R. Ryan, *Organometallics*, *3* (1984) 1434; (b) P. Ewing and L.J. Farrugia, *Organometallics*, *8* (1989) 1665.
[15] D.J. Taube and P.C. Ford, *Organometallics*, *5* (1986) 99.
[16] (a) L. Chen and A.J. Pöe, *Can. J. Chem.*, 67 (1989) 1924; (b) M.I. Bruce, M.J. Liddell, O. Bin Shawkataly, I. Bytheway, B.W. Skelton and A.H. White, *J. Organomet. Chem.*, 369 (1989) 217; (c) G. Foulds, B.F.G. Johnson and J. Lewis, *J. Organomet. Chem.*, 296 (1985) 147; (d) B.F.G. Johnson, *Inorg. Chim. Acta*, 115 (1986) L39; (e) M.F. Desrosiers, D.A. Wink, R. Trautman, A.E. Friedman and P.C. Ford, *J. Am. Chem. Soc.*, 108 (1986) 1917; (f) T. Venäläinen, J. Pursianinen and T.A. Pakkanen, *J. Chem. Soc., Chem. Commun.*, (1985) 1348; (g) M.F. Desrosiers, D.A. Wink and P.C. Ford, *Inorg. Chem.*, 24 (1985) 1; (h) M. Anstock, D. Taube, D.C. Gross and P.C. Ford, *J. Am. Chem. Soc.*, 106 (1984) 3696.
[17] D.F. Shriver and M.A. Drezdzon, *The Manipulation of Air-Sensitive Compounds*, 2nd edn.; Wiley, New York, 1986.
[18] A.J. Gordon and R.A. Ford, *The Chemist's Companion*, Wiley, New York, 1972.
[19] G.B. Karet, E.J. Voss and D.F. Shriver, *Inorg. Synth.*, submitted, for publication.
[20] G. Suss-Fink, *Inorg. Synth.*, 24 (1986) 168.
[21] D.C. Moody and R.R. Ryan, *J. Chem. Soc., Chem. Commun.*, (1980) 1230.
[22] (a) J. Haase and M. Winnewisser, *Z. Naturforsch., A*23 (1968) 61; (b) B. Post, R.S. Schwartz and I. Fankuchen, *Acta Crystallogr.*, *5* (1952) 372; (c) Y. Morino, Y. Kikuchi, S. Saito and E. Hiroto, *J. Mol. Spectrosc.*, 13 (1964) 95.
[23] G.J. Kubas, *Inorg. Chem.*, 18 (1979) 182.
[24] L.S. Farrugia and S.E. Rae, *Organometallics*, 22 (1992) 196.
[25] J.A. Hriljac, *PhD. Thesis*, Northwestern University, 1987.
[26] C.P. Horwitz and D.F. Shriver, *Adv. Organomet. Chem.*, 23 (1984) 219.
[27] A.D. Burrows, D.M.P. Mingos and H.R. Powell, *J. Chem. Soc., Dalton Trans.*, (1992) 261.